Bioorganic & Medicinal Chemistry Letters 21 (2011) 1064–1068

Contents lists available at ScienceDirect

Bioorganic & Medicinal Chemistry Letters

journal homepage: www.elsevier.com/locate/bmcl

# $^{99m}$Tc- and Re-labeled 6-dialkylamino-2-naphthylethylidene derivatives as imaging probes for β-amyloid plaques

Mengchao Cui, Ruikun Tang, Zijing Li, Huiying Ren, Boli Liu *

*Key Laboratory of Radiopharmaceuticals (Beijing Normal University), Ministry of Education, College of Chemistry, Beijing Normal University, Beijing 100875, PR China*

ARTICLE INFO

*Article history:*
Received 3 July 2010
Revised 30 October 2010
Accepted 20 November 2010
Available online 4 December 2010

*Keywords:*
Alzheimer's disease
β-Amyloid
Technium-99m
Imaging agent

ABSTRACT

Based on the conjugate strategy, two neutral $^{99m}$Tc labeled 2-(1-(6-(dialkylamino)naphthalen-2-yl)ethylidene)malononitrile (DDNP) and 1-(6-(dialkylamino)naphthalen-2-yl)ethanone (ENE) derivatives, and their corresponding rhenium complexes were synthesized. In vitro fluorescent staining indicated that the corresponding rhenium derivatives selectively stained the β-amyloid (Aβ) plaques in the brain sections of AD model mice with low background. Compared with FDDNP and FENE, the affinities of the corresponding rhenium derivatives to Aβ aggregates decreased about 10–14-fold. In vivo biodistribution experiments in normal mice showed that $^{99m}$Tc-MAMA-ENE displayed medium initial brain uptake (0.65 %ID/g at 2 min) with a reasonable washout from the brain (0.19 %ID/g at 2 h) while $^{99m}$Tc-MAMA-DDNP showed a low brain uptake (0.28 %ID/g at 2 min). Further optimize these $^{99m}$Tc-labeled tracers in order to improve their binding affinities to Aβ plaques and diffusion through the blood brain barrier may generate useful imaging agents for SPECT.



Senile plaques (SPs) composed of misfolded β-amyloid (Aβ) peptides and neurofibrillary tangles (NFTs) made of hyperphosphorylated tau aggregates are two of the pathological hallmarks of AD.[1,2] Development of imaging probes targeting amyloid plaques or neurofibrillary tangles for positron emission tomography (PET) and single photon emission computed tomography (SPECT) will be crucial for early diagnosis of AD.[3] Based on the structure of Thioflavin-T and Congo red, several types of Aβ imaging agents have been synthesized and evaluated in the past decade. Some of them have so far reached clinical stage, such as [$^{18}$F]FDDNP,[4–6] [$^{11}$C]PIB,[7,8] [$^{11}$C]SB-13,[9,10] [$^{11}$C]BF-227,[11] [$^{18}$F]AV-45,[12,13] and [$^{123}$I]IMPY.[14–16] Although the clinical evaluations of these agents are encouraging, $^{11}$C and $^{18}$F have their distinct features, such as short half-life and high cost of nuclear production from cyclotron, which decreased the potential use of these agents in clinical. Among the medical radio-nuclides, $^{99m}$Tc ($T_{1/2}$ = 6 h, 140 keV) is the most widely used radioisotope for in vivo diagnostic imaging in SPECT with some favorable factors: it can be easily produced from a $^{99}$Mo/$^{99m}$Tc generator, the medium gamma-ray energy emitted by $^{99m}$Tc (140 keV) is suitable for gamma camera detection and the half-life is compatible with the biological localization and residence time required for imaging.[17] Thus, the successful developing of $^{99m}$Tc labeled imaging agents for Aβ plaques would provide a simple and widespread method for clinical diagnosis of AD using SPECT. However, in order to introduce the transition metal $^{99m}$Tc to an organic molecule, a chelating structure is obligatory. Two broad strategies (conjugate approach or integrated approach) have been used in the design of $^{99m}$Tc-labeled Aβ imaging agents in order not to reduce the affinity and selectivity or decrease the brain uptake.[18] Previous studies of $^{99m}$Tc-labeled Congo Red and Chrysamine G derivatives based on the conjugate strategy have been reported.[19,20] But these $^{99m}$Tc complexes are both too large and charged molecules and therefore, cannot penetrate the blood-brain barrier (BBB). Attempts to prepare small, neutral and more lipophilic ligands such as derivatives of benzothiazole aniline (BTA),[21–23] stilbene,[24] flavone[25], chaclone,[26] and biphenyl[27] labeled with $^{99m}$Tc have been reported (Fig. 1). A biphenyl derivative based on the integrated strategy, showed high initial brain uptakes, with a brain uptake up to 1.18% dose/organ at 2 min, but it failed to bind to the Aβ plaques in the postmortem human brain tissue of patients with confirmed AD.[27] Through the conjugate strategy, our group reported that $^{99m}$Tc-labeled BTA derivatives using monoamide–monoamine (MAMA) as the chelator, displayed high brain uptake in normal mice (1.34 %ID/g at 2 min).[28]

[$^{18}$F]FDDNP and its analog [$^{18}$F]FENE are two small molecules with compact naphthalene core and high affinity for both Aβ plaques and neurofibrillary tangles.[4] Previous reports indicated that they bind to Aβ aggregates on a distinct binding site.[29] The aim of this study was to synthesize neutral $^{99m}$Tc/rhenium labeled derivatives of FDDNP and FENE, and to evaluate their biological characteristics.

The synthesis of the $^{99m}$Tc- and Re-labeled 6-dialkylamino-2-naphthylethylidene derivatives is outlined in Scheme 1. Compounds **3** and **5** were obtained according to the literature previously reported.[30] Then bromination of the hydroxyl group

* Corresponding author. Tel./fax: +86 010 5880 8891.
*E-mail address:* liuboli@bnu.edu.cn (B. Liu).

0960-894X/$ - see front matter © 2010 Elsevier Ltd. All rights reserved.
doi:10.1016/j.bmcl.2010.11.096

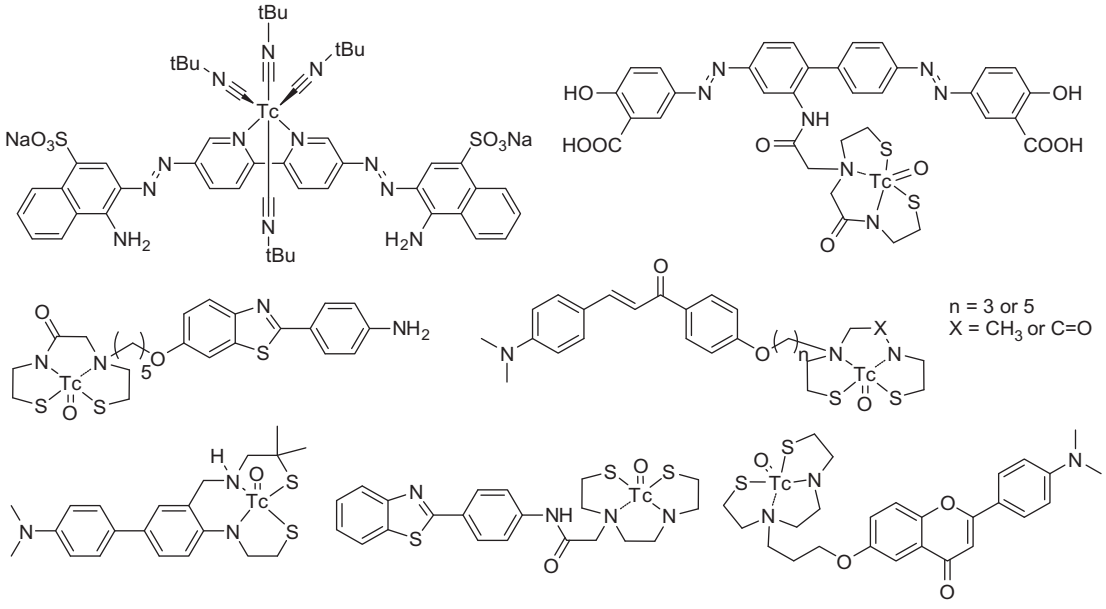


**Figure 1.** Structures of $^{99m}$Tc-labeled amyloid imaging probes.

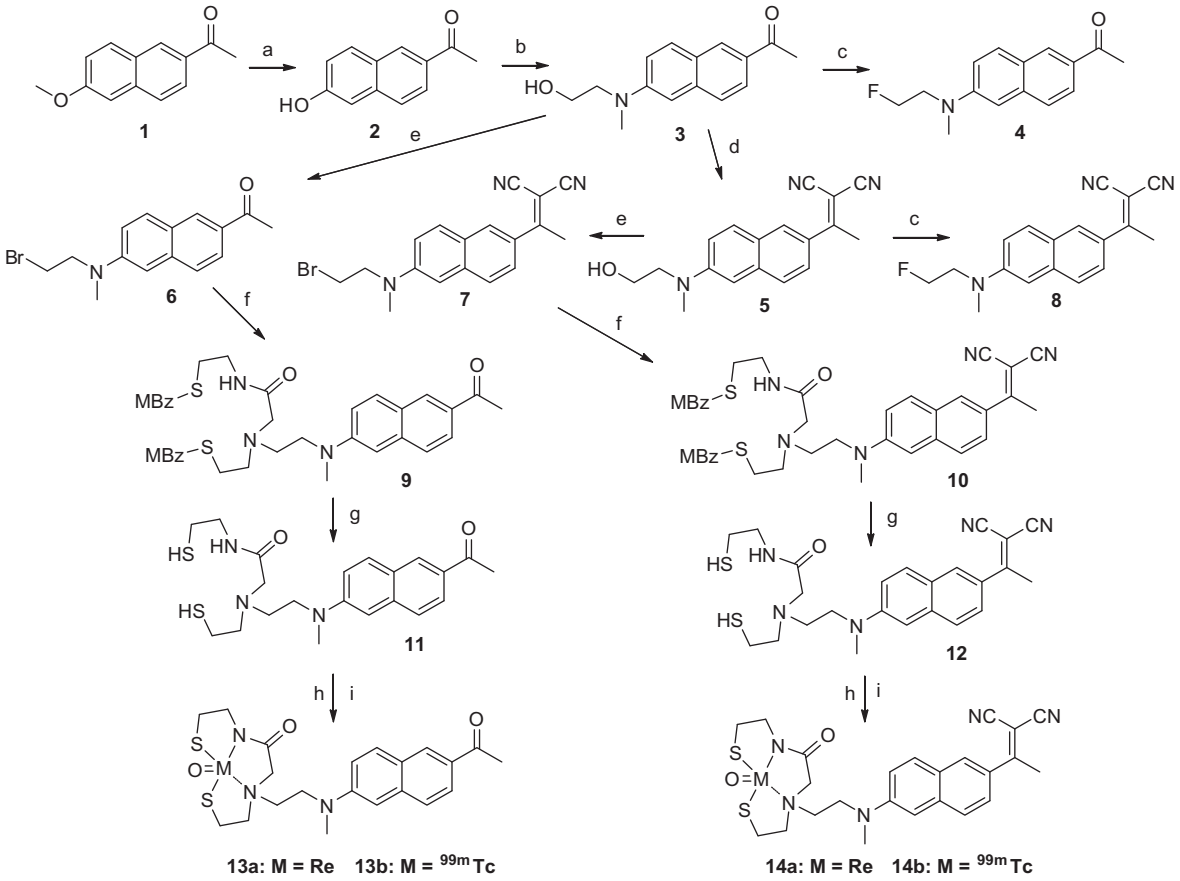


**Scheme 1.** Reagents and conditions: (a) 37% HCl, reflux; (b) $CH_3NHCH_2CH_2OH$, $Na_2S_2O_5$, $H_2O$, 140 °C; (c) DAST, $CH_2Cl_2$, −78 to 0 °C; (d) $CH_2(CN)_2$, pyridine, 110 °C; (e) $CH_2Cl_2$, NBS, $PPh_3$, 0–25 °C; (f) acetonitrile, MAMA-MBz (*p*-methoxy benzyl), DIEA, reflux; (g) anisole, $CH_3SO_3H$, TFA, 0–25 °C; (h) $ReOCl_3(PPh_3)_2$, $CH_3OH$, $CH_2Cl_2$, 90 °C; (i) $^{99m}$Tc-GH, 100 °C.

was performed in $CH_2Cl_2$ with NBS, giving **6** and **7** with the yields of 79.3% and 76.7%, respectively. Then the compound **6** and **7** were conjugated to MAMA (thiol groups were protected with *p*-methoxy benzyl to prevent oxidation) in $CH_3CN$ with *N*,*N*-diisopropylethylamine (DIEA) as base to generate compound **9** (yield 32.3%) and **10** (yield 25.3%). After deprotection of the thiol groups using trifluoro acetic acid (TFA) and $CH_3SO_3H$ at 0 °C, precursor **11** and **12** were obtained with the yields of 42.0% and 57.0%, respectively.

Fluorinated compounds **4** (FENE) and **8** (FDDNP) were also obtained from **3** and **5** reacted with diethylamino sulfur trifluoride (DAST).

Rhenium complexes generally display similar physical and biodistributional properties to those of technetium complexes and have been normally adopted as non-radioactive surrogates for $^{99m}$Tc complexes for structure identification. In this study, the corresponding rhenium complexes **13a** (yield 23.2%) and **14a** (yield 20.4%) were obtained from **11** and **12** by reacting with $ReOCl_3(PPh_3)_2$ in $CH_2Cl_2$.

$^{99m}$Tc-labeled complexes **13b** and **14b** were prepared by ligand exchange reaction employing the precursor $^{99m}$Tc-glucoheptonate (GH), after heating in boiling water bath for 15 min. The labeling yields detected by radio-HPLC were higher than 95%. After purification by HPLC, the radio-chemical purities of **13b** and **14b** were both greater than 98%. They were stable in saline more than 6 h at room temperature. The radio-chemical identities of the $^{99m}$Tc labeled tracers were verified by co-elution with the corresponding rhenium complexes on HPLC profiles (See in Supplementary data).

The affinity of rhenium complexes **13a** and **14a** for $A\beta_{1-42}$ aggregates was determined by competition binding assay using [$^{125}$I]IMPY as radio-ligand, FDDNP and FENE were also screened using the same system for comparison. The inhibition curves shown in Figure 2 suggest that the rhenium complexes inhibit the binding of [$^{125}$I]IMPY in a dose-dependent manner. However, their binding affinities for $A\beta_{1-42}$ aggregates were relative lower with the $K_i$ values in the micromolar range. Under the same experimental conditions FDDNP and FENE also showed low binding affinities to Aβ aggregates (Table 1). The reason may be due to the different binding sites between IMPY and FDDNP. Compared with FDDNP and FENE, the affinities of the corresponding rhenium complexes to Aβ aggregates decreased about 10–14-fold, which indicate that introducing the oxorhenium core chelated by a MAMA moiety through conjugate approach reduce the binding affinity.

The specific nature of rhenium complexes **13a** and **14a** to Aβ plaques was investigated by neuropathological staining with the brain sections of a 12-month-old AD transgenic model (Tg-C57), which encoded a double mutant form of APP and PS1. Many Aβ plaques were clearly stained by these compounds with low background (Fig. 3A and D). The similar pattern of Aβ plaques was also stained with Thioflavin-S using the adjacent brain sections (Fig. 3B and E). No plaques were found in control sections (Fig. 3C and F). The results indicated that these derivatives show specific binding to Aβ plaques. Because of the similar characteristics of technetium and rhenium, $^{99m}$Tc-labeled complexes could also bind to Aβ plaques.

It is believed that small molecular size (<600 Da) and moderate lipophilicity (Log *P* values in the range of 1–3) are two of the major factors for BBB penetration.[29,31] The partition coefficients of the

**Table 1**
Inhibition constants ($K_i$, μM) for the binding to $A\beta_{1-42}$ aggregates versus [$^{125}$I]IMPY and HPLC profiles

| Compound | $K_i$[a] (μM) | Retention time (min) |
|---|---|---|
| **4** (FENE) | 0.39 ± 0.05 | n.d. |
| **13a** | 3.65 ± 0.49 | 25.83 |
| **13b** | n.d. | 26.15 |
| **8** (FDDNP) | 0.33 ± 0.09 | n.d. |
| **14a** | 4.64 ± 0.77 | 24.92 |
| **14b** | n.d. | 25.35 |

[a] Measured in triplicate with results given as the mean ± SD.

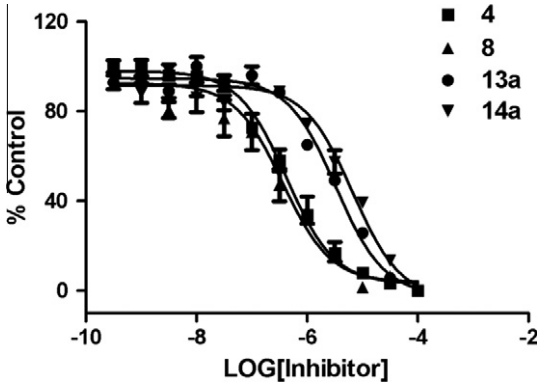


**Figure 3.** Inhibition curves of **4**, **8**, **13a** and **14a** for the binding to aggregates of $A\beta_{1-42}$ versus [$^{125}$I]IMPY.

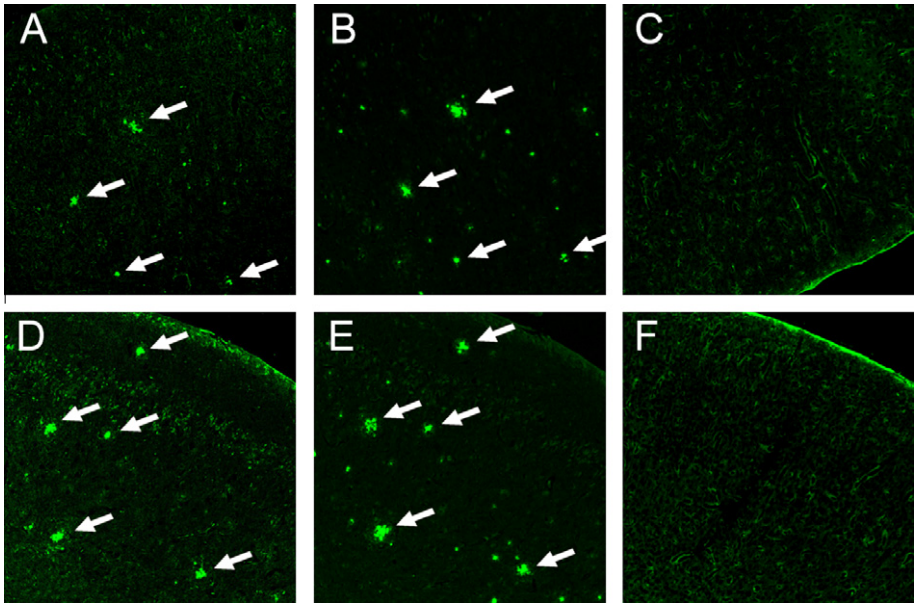


**Figure 2.** Fluorescent staining of **13a** (A) and **14a** (D) on the brain slices (5 μm) of a AD transgenic model (APP/PS1) and wild control (C and F). Plaques were also confirmed by the staining of the adjacent sections with Thioflavin-S (B and E).

**Table 2**
Biodistribution experiments of **13b** and **14b** in normal mice[a]

| Tissue | Time after injection (min) | | | | |
|---|---|---|---|---|---|
| | 2 | 10 | 30 | 60 | 120 |
| **13b** Log *D* = 1.89 ± 0.04 | | | | | |
| Blood | 5.81 ± 0.95 | 2.55 ± 0.81 | 2.07 ± 0.19 | 1.64 ± 0.27 | 1.22 ± 0.38 |
| Heart | 6.88 ± 1.03 | 3.84 ± 0.56 | 2.85 ± 0.25 | 2.26 ± 0.52 | 1.35 ± 0.4 |
| Liver | 9.31 ± 0.96 | 12.49 ± 1.85 | 13.85 ± 1.25 | 12.79 ± 2.97 | 8.63 ± 2.09 |
| Spleen | 2.78 ± 0.41 | 2.98 ± 0.36 | 2.51 ± 0.3 | 2.13 ± 0.21 | 1.21 ± 0.23 |
| Lung | 8.27 ± 2.03 | 4.31 ± 0.48 | 3.17 ± 0.13 | 2.66 ± 0.4 | 1.50 ± 0.34 |
| Kidney | 6.56 ± 0.63 | 4.67 ± 0.71 | 4.12 ± 0.62 | 3.66 ± 0.52 | 2.24 ± 0.53 |
| Brain | 0.65 ± 0.09 | 0.60 ± 0.04 | 0.44 ± 0.02 | 0.36 ± 0.06 | 0.19 ± 0.03 |
| **14b** Log *D* = 1.70 ± 0.02 | | | | | |
| Blood | 6.35 ± 0.59 | 2.43 ± 0.39 | 1.71 ± 0.31 | 1.14 ± 0.13 | 0.73 ± 0.08 |
| Heart | 10.77 ± 1.1 | 5.47 ± 0.43 | 2.94 ± 0.46 | 1.86 ± 0.29 | 1.25 ± 0.3 |
| Liver | 18.31 ± 3.23 | 21.12 ± 3.83 | 16.95 ± 1.89 | 15.48 ± 3.63 | 13.9 ± 3.61 |
| Spleen | 3.57 ± 0.44 | 3.21 ± 0.35 | 2.34 ± 0.29 | 1.50 ± 0.23 | 1.08 ± 0.23 |
| Lung | 10.59 ± 1.74 | 4.67 ± 0.85 | 3.24 ± 0.43 | 2.29 ± 0.31 | 1.47 ± 0.21 |
| Kidney | 11.01 ± 1.88 | 8.56 ± 0.84 | 5.93 ± 0.87 | 4.18 ± 0.47 | 3.14 ± 0.74 |
| Brain | 0.28 ± 0.03 | 0.21 ± 0.02 | 0.17 ± 0.03 | 0.12 ± 0.02 | 0.10 ± 0.04 |

[a] All data are expressed as the mean percentage ($n = 4$) of the injected dose per gram of wet tissue (%ID/g) ± the standard deviation of the mean.

radiotracers were determined using a described procedure,[32] Log *D* values of **13b** and **14b** were 1.70 ± 0.02 and 1.89 ± 0.04, respectively, which are in a good range for BBB penetration. As their molecular weight does not exceed 600 Da, **13b** and **14b** are expected to pass through the BBB and show better brain uptake.

In vivo biodistribution experiment was carried out on ICR normal mice (weight 18–22 g). A saline solution (100 μL) containing 7 μCi purified radiotracer was injected directly into the tail vein. The mice were sacrificed at various time points after intravenous administration. The biodistribution data are shown in Table 2. Complex **13b** displayed a medium initial brain uptake (0.65 %ID/g at 2 min pi) and a reasonable washout of the radioactivity from the brain (0.19 %ID/g at 2 h pi) while **14b** showed a low brain uptake (0.28 %ID/g at 2 min). Although the lipophilicity of **13b** and **14b** was in a moderate range and their molecular weight did not exceed the threshold of 600 Da, they cannot cross the BBB to a sufficient degree, since the brain uptake was also dependent on other factors, such as hydrogen bonding, percentage of intact tracer in vivo, etc. Compared with that of the $^{99m}$Tc-labeled BTA reported by our group,[28] the initial brain uptake of these $^{99m}$Tc-labeled DDNP derivatives appears insufficient for in vivo imaging. Therefore, further optimizations are needed to improve the pharmacokinetics of these $^{99m}$Tc-labeled DDNP derivatives in vivo.

In conclusion, two $^{99m}$Tc-labeled DDNP derivatives and their corresponding rhenium complexes were successfully synthesized through the conjugate approach. In experiments in vitro, the rhenium complexes **13a** and **14a** showed lower affinities for Aβ aggregates than FDDNP. However, both of them can bind to Aβ plaques in the brain sections of AD transgenic mouse. Due to the similar chemical and physical properties between rhenium and technetium, the $^{99m}$Tc-labeled tracers **13b** and **14b** are expected to retain the binding affinity to Aβ plaques. Despite the fact that **13b** and **14b** displayed moderate lipophilicity and their molecular weights were less than 600 Da, in vivo biodistribution studies of **13b** exhibited a medium initial brain uptake while **14b** showed lower brain uptake. These results imply that these $^{99m}$Tc-labeled DDNP derivatives probably require further refinement in order to improve their diffusion through the BBB and provide some useful information for the development of $^{99m}$Tc-labeled probes for β-amyloid imaging.

## Acknowledgments

We thank Dr. Lianfeng Zhang (Institute of Laboratory Animal Science, Chinese Academy of Medical Sciences and Comparative Medicine Center of Peking Union Medical College) for kindly providing the Paraffin-embedded brain sections of Tg-C57 mouse and Dr. Xiaoyan Zhang (College of Life Science, Beijing Normal University) for assistance in the in vitro neuropathological staining. This work was funded by NSFC (20871021).

## Supplementary data

Supplementary data (procedure for the preparation of $^{99m}$Tc- and Re-labeled DDNP derivatives, in vitro binding assay, fluorescent staining and biodistribution experiments) associated with this article can be found, in the online version, at doi:10.1016/j.bmcl.2010.11.096.

## References and notes

1. Selkoe, D. J. *JAMA* **2000**, *283*, 1615.
2. Hardy, J. A.; Selkoe, D. J. *Science* **2002**, *297*, 353.
3. Mathis, C. A.; Wang, Y.; Klunk, W. E. *Curr. Pharm. Des.* **2004**, *10*, 1469.
4. Agdeppa, E. D.; Kepe, V.; Liu, J.; Flores-Torres, S.; Satyamurthy, N.; Petric, A.; Cole, G. M.; Small, G. W.; Huang, S. C.; Barrio, J. R. *J. Neurosci.* **2001**, *21*, RC189.
5. Shoghi-Jadid, K.; Small, G. W.; Agdeppa, E. D.; Kepe, V.; Ercoli, L. M.; Siddarth, P.; Read, S.; Satyamurthy, N.; Petric, A.; Huang, S. C.; Barrio, J. R. *Am. J. Geriatr. Psychiatry* **2002**, *10*, 24.
6. Small, G. W.; Kepe, V.; Ercoli, L. M.; Siddarth, P.; Bookheimer, S. Y.; Miller, K. J.; Lavretsky, H.; Burggren, A. C.; Cole, G. M.; Vinters, H. V.; Thompson, P. M.; Huang, S. C.; Satyamurthy, N.; Phelps, M. E.; Barrio, J. R. *N. Eng. J. Med.* **2006**, *355*, 2652.
7. Mathis, C. A.; Wang, Y.; Holt, D. P.; Huang, G. F.; Debnath, M. L.; Klunk, W. E. *J. Med. Chem.* **2003**, *46*, 2740.
8. Klunk, W. E.; Engler, H.; Nordberg, A.; Wang, Y.; Blomqvist, G.; Holt, D. P.; Bergstrom, M.; Savitcheva, I.; Huang, G. F.; Estrada, S.; Ausen, B.; Debnath, M. L.; Barletta, J.; Price, J. C.; Sandell, J.; Lopresti, B. J.; Wall, A.; Koivisto, P.; Antoni, G.; Mathis, C. A.; Langstrom, B. *Ann. Neurol.* **2004**, *55*, 306.
9. Verhoeff, N. P.; Wilson, A. A.; Takeshita, S.; Trop, L.; Hussey, D.; Singh, K.; Kung, H. F.; Kung, M. P.; Houle, S. *Am. J. Geriatr. Psychiatry* **2004**, *12*, 584.
10. Ono, M.; Wilson, A.; Nobrega, J.; Westaway, D.; Verhoeff, P.; Zhuang, Z. P.; Kung, M. P.; Kung, H. F. *Nucl. Med. Biol.* **2003**, *30*, 565.
11. Kudo, Y.; Okamura, N.; Furumoto, S.; Tashiro, M.; Furukawa, K.; Maruyama, M.; Itoh, M.; Iwata, R.; Yanai, K.; Arai, H. *J. Nucl. Med.* **2007**, *48*, 553.
12. Choi, S. R.; Golding, G.; Zhuang, Z. P.; Zhang, W.; Lim, N.; Hefti, F.; Benedum, T. E.; Kilbourn, M. R.; Skovronsky, D.; Kung, H. F. *J. Nucl. Med.* **2009**, *50*, 1887.
13. Kung, H. F.; Choi, S. R.; Qu, W. C.; Zhang, W.; Skovronsky, D. *J. Med. Chem.* **2010**, *53*, 933.
14. Kung, M. P.; Hou, C.; Zhuang, Z. P.; Zhang, B.; Skovronsky, D.; Trojanowski, J. Q.; Lee, V. M.; Kung, H. F. *Brain Res.* **2002**, *956*, 202.
15. Zhuang, Z. P.; Kung, M. P.; Wilson, A.; Lee, C. W.; Plossl, K.; Hou, C.; Holtzman, D. M.; Kung, H. F. *J. Med. Chem.* **2003**, *46*, 237.
16. Newberg, A. B.; Wintering, N. A.; Plossl, K.; Hochold, J.; Stabin, M. G.; Watson, M.; Skovronsky, D.; Clark, C. M.; Kung, M. P.; Kung, H. F. *J. Nucl. Med.* **2006**, *47*, 748.
17. Jurisson, S. S.; Lydon, J. D. *Chem. Rev.* **1999**, *99*, 2205.
18. Hom, R. K.; Katzenellenbogen, J. A. *Nucl. Med. Biol.* **1997**, *24*, 485.
19. Zhen, W.; Han, H.; Anguiano, M.; Lemere, C. A.; Cho, C. G.; Lansbury, P. T. *J. Med. Chem.* **1999**, *42*, 2805.

20. Dezutter, N. A. D. G.; de Groot, T. J.; Bormans, G. M.; Verbruggen, A. M.; Dom, R. J. *Eur. J. Nucl. Med. Mol. Imaging* **1999**, *26*, 1392.
21. Serdons, K.; Verduyckt, T.; Cleynhens, J.; Terwinghe, C.; Mortelmans, L.; Bormans, G.; Verbruggen, A. *Bioorg. Med. Chem. Lett.* **2007**, *17*, 6086.
22. Serdons, K.; Verduyckt, T.; Cleynhens, J.; Terwinghe, C.; Bormans, G.; Verbruggen, A. *J. Labelled Compd. Radiopharm.* **2008**, *51*, 357.
23. Lin, K. S.; Debnath, M. L.; Mathis, C. A.; Klunk, W. E. *Bioorg. Mde. Chem. Lett.* **2009**, *19*, 2258.
24. Zhuang, Z. P.; Kung, M. P.; Hou, C.; Kung, H. F. *J. Labelled Compd. Radiopharm.* **2005**, *48*, S251.
25. Ono, M.; Ikeoka, R.; Watanabe, H.; Kimura, H.; Fuchigami, T.; Haratake, M.; Saji, H.; Nakayama, M. *Bioorg. Med. Chem. Lett.* **2010**, *20*, 5743.
26. Ono, M.; Ikeoka, R.; Watanabe, H.; Kimura, H.; Fuchigami, T.; Haratake, M.; Saji, H.; Nakayama, M. *ACS Chem. Neurosci.* **2010**, *1*, 598.
27. Zhuang, Z. P.; Kung, M. P.; Hou, C.; Ploessl, K.; Kung, H. F. *Nucl. Med. Biol.* **2005**, *32*, 171.
28. Chen, X. J.; Yu, P. R.; Zhang, L. F.; Liu, B. L. *Bioorg. Med. Chem. Lett.* **2008**, *18*, 1442.
29. Cai, L. S.; Innis, R. B.; Pike, V. W. *Curr. Med. Chem.* **2007**, *14*, 19.
30. Liu, J.; Kepe, V.; Zabjek, A.; Petric, A.; Padgett, H. C.; Satyamurthy, N.; Barrio, J. R. *Mol. Imaging Biol.* **2007**, *9*, 6.
31. Furumoto, S.; Okamura, N.; Iwata, R.; Yanai, K.; Arai, H.; Kudo, Y. *Curr. Top. Med. Chem.* **2007**, *7*, 1773.
32. Wu, C. Y.; Wei, J. J.; Gao, K. Q.; Wang, Y. M. *Bioorg. Med. Chem.* **2007**, *15*, 2789.